The Effect and Role of Carbon Atoms in Poly(β-amino ester)s for DNA Binding and Gene Delivery

Corey J. Bishop,[†,∞] Tiia-Maaria Ketola,[‡] Stephany Y. Tzeng,[†,∞] Joel C. Sunshine,[†,∞] Arto Urtti,[§] Helge Lemmetyinen,[‡] Elina Vuorimaa-Laukkanen,[‡] Marjo Yliperttula,[∥] and Jordan J. Green*[†,¶,∞,#]

[†]Department of Biomedical Engineering, the [#]Department of Ophthalmology, the [∞]Translational Tissue Engineering Center, and the [¶]Institute for Nanobiotechnology, Johns Hopkins University School of Medicine, 400 North Broadway, Baltimore, Maryland 21231, United States

[‡]Department of Chemistry and Bioengineering, Tampere University of Technology, P.O. Box 541, FI-33101 Tampere, Finland

[§]Division of Biopharmacy and Pharmacokinetics and [∥]Centre for Drug Research, Faculty of Pharmacy, University of Helsinki, Viikinkaari 5E, 00014 Helsinki, Finland

Ⓢ Supporting Information

ABSTRACT: Polymeric vectors for gene delivery are a promising alternative for clinical applications, as they are generally safer than viral counterparts. Our objective was to further our mechanistic understanding of polymer structure–function relationships to allow the rational design of new biomaterials. Utilizing poly(β-amino ester)s (PBAEs), we investigated polymer–DNA binding by systematically varying the polymer molecular weight, adding single carbons to the backbone and side chain of the monomers that constitute the polymers, and varying the type of polymer end group. We then sought to correlate how PBAE binding affects the polyplex diameter and ζ potential, the transfection efficacy, and its associated cytotoxicity in human breast and brain cancer cells in vitro. Among other trends, we observed in both cell lines that the PBAE–DNA binding constant is biphasic with the transfection efficacy and that the optimal values of the binding constant with respect to the transfection efficacy are in the range $(1-6) \times 10^4 \ M^{-1}$. A binding constant in this range is necessary but not sufficient for effective transfection.
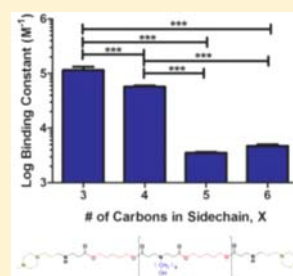
INTRODUCTION

Inheritable diseases and cancer can result from inactive genes (i.e., CFTR in cystic fibrosis or P53 as a tumor suppressor).[1,2] Delivering DNA and small hairpin RNA to encode and generate a functional copy or to inhibit mRNA expression of a nonfunctioning protein can potentially treat and cure many genetic diseases. Viruses have been used as delivery vectors because they are highly efficient in nucleic acid delivery, but they can cause insertional mutagenesis, immunogenic responses, and toxicity.[3] The safety and efficacy of the viral vectors depend on the viral vector type, route of administration, and therapeutic target. To date, only two gene therapy formulations have been approved, one by the State Food and Drug Administration of China (2003) and the other by the European Medicines Agency (2012); there are still no U.S. Food and Drug Administration-approved gene therapies.[4] Degradable cationic polymers are an attractive alternative to viruses, as they are generally safer, are easier to manufacture and mass produce, and have more functional capabilities than viruses.[5] Varying a polymer's structure and functional groups allows one to optimize the nucleic acid delivery properties while minimizing toxicity levels.[6] High-throughput analyses of combinatorial biomaterial libraries allow a vast number of polymers to be screened, but rational design of structure to control function would be more efficient.[7,8]

We are interested in evaluating polymer structure–function relationships to further our mechanistic understanding of polymeric materials for nonviral gene delivery and improve their performance (Scheme 1). We previously investigated poly(β-amino esters) (PBAEs) as biodegradable cationic polymers capable of promoting gene delivery to various types of cells.[9−11] These polymers are promising because of their ability to condense DNA into nanoparticles containing many

Scheme 1. Nanoparticle Formulation and Extracellular and Intracellular Barriers for Successful Gene Delivery
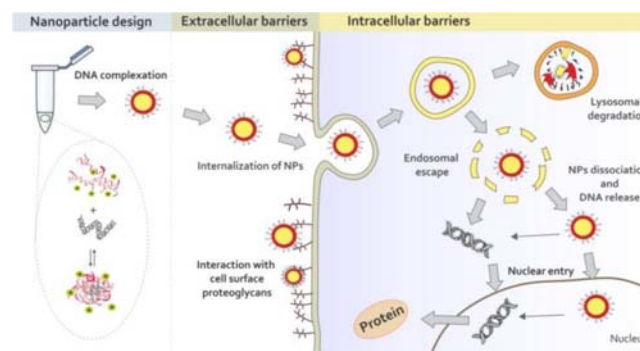
plasmids per particle,[12] facilitate cellular uptake,[13] and mediate endosomal escape.[14,15] Certain PBAE nanoparticles have been shown to be effective for in vivo gene delivery in the eye[16] and to tumors.[17] Despite this progress, the efficiency of gene delivery using polymers remains lower than that for viral delivery. One challenge in evaluating and optimizing polymer structure is that synthetic polymers can be polydisperse, with variable extents of reaction and molecular weight heterogeneity.[18−20] Isolating precise polymer structures with uniform molecular weight is key for enabling the evaluation of polymer structure.

The interactions between a cationic polymer and DNA are critical for facilitating DNA protection, nanoparticle formation, cellular uptake, and subsequent DNA release.[21,22] Anionic phosphate groups on the DNA associate with and bind to positively charged amine groups on cationic polymers, resulting in nucleic acid condensation and protection. This is important because the degradation half-life of naked DNA in the presence of serum is on the order of minutes.[23] Binding with a cationic carrier (i.e., a polymer) can substantially increase the nucleic acid half-life.[24,25] An optimal DNA carrier system should bind, condense, and protect DNA in the extracellular space but release DNA effectively within cells. The design of such systems requires proper understanding of the binding between DNA and polycations.[26,27]

In this work, we used time-resolved fluorescence spectroscopy,[28,29] a new approach for probing polymer−DNA interactions and binding quantitatively. Here we report the results of our systematic investigation of binding properties of DNA and monodisperse, size-fractionated PBAEs with differential structures. In particular, we investigated series of polymers in which the following were varied: molecular weight; the number of carbons in the backbone, which varied the amine density and hydrophobicity; the number of carbons in the side chain, which varied the distance of a hydroxyl group from the backbone and its hydrophobicity; and the end-cap type [primary, secondary, or tertiary amine or no end cap (diacrylate-terminated)]. The effects of these small changes in the polymer structure were characterized by fluorescence spectroscopy and gene delivery efficacy in human brain cancer cells and human breast cancer cells in vitro.[30] The experimental procedures, including materials and methods and the naming convention for the polymers, can be found in the Supporting Information.

■ RESULTS AND DISCUSSION

Polymer Synthesis and Fractionation. In the 447 polymer series with varying molecular weight (447 Low M_w, 447 Med M_w, and 447 High M_w), the weight-average molecular weights (M_w) were 10.3, 14.7, and 91.6 kDa, respectively, and the polydispersity index (PDI) increased as M_w increased (PDI = 1.3, 1.4, and 2.9, respectively) (Table S1 in the Supporting Information). The average M_w's for the groups in which the backbone, side chain, and end caps were varied were 10 ± 1, 13 ± 2, and 10.9 ± 0.7 kDa, respectively, and the corresponding average PDIs were 1.3 ± 0.1, 1.3 ± 0.1, and 1.34 ± 0.09 (Table S1). The molecular weights of the polymers were determined by gel-permeation chromatography (GPC) (Figure 1). The molecular weights varied considerably for the 447 molecular weight series but were similar for the other polymers. The similarity of the M_w values and the narrow PDIs of the comparable polymers with small differences in the backbone, side chain, and end cap allowed comparisons between the
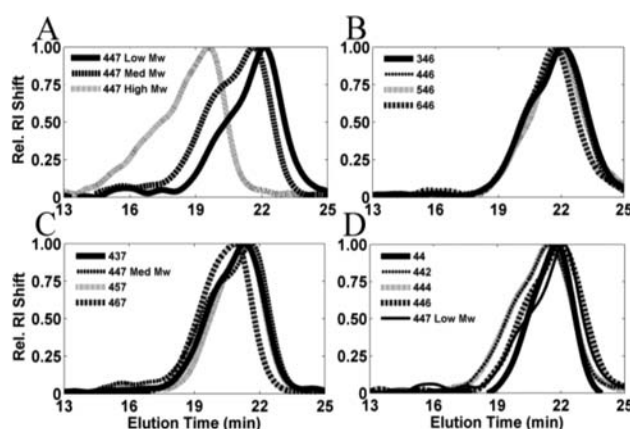

Figure 1. GPC curves of fractionated polymers [relative refractive index (RI) shift (mV/max mV) vs elution time (min)] for groups with varying (A) molecular weight (Low, Med, and High), (B) backbone, (C), side chain, and (D) end caps.

groups and ensured that differences were due to the monomer type as opposed to M_w or size heterogeneity.

Representative ^{1}H NMR spectra of polymers 44, 442, 444, 446, and 447 can be found in Figure S1 in the Supporting Information.[6]

Binding Constants for Polyplex Formation. The polyplex formation can be monitored by plotting the proportion of bound DNA (B in eq 5 in the Supporting Information) against the concentration of amine. As an example, the plot for polymer 442 is shown in Figure 2. The
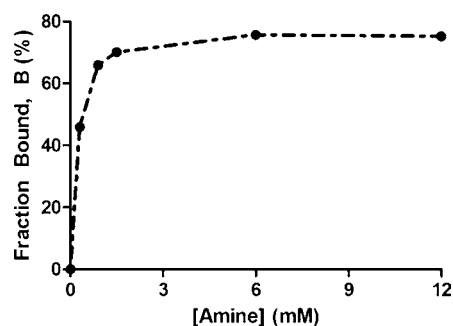

Figure 2. Fraction of bound DNA as a function of amine concentration for polymer 442.

proportion of bound DNA increased with increasing polymer concentration until it reached a saturation limit of approximately 76% at a polymer/DNA weight/weight (w/w) ratio of 24. Most of the PBAE polymers saturated close to 80%. The saturation limits for polymers 44 and 346 were 60% and 96%, respectively. Polymers with negative cooperativity typically have saturation less than 100%, whereas polymers with high positive cooperativity saturate near 100%.

The Hill plots for the 447 molecular weight series are shown in Figure 3A. Similar linear curves with negative cooperativity (Table S1 in the Supporting Information) were obtained for all of the polymers except polymer 646 (Figure 3B−D). The fact that the Hill plots for most of the polymers entailed negative cooperativity and the fact that the bound fraction for most of the polymers saturated close to 80% are in agreement.

While most of the polymers showed a single linear Hill plot, varying the polymer backbone structure (646) enabled a biphasic response (Figure 3B). Polymer 646's Hill plot is
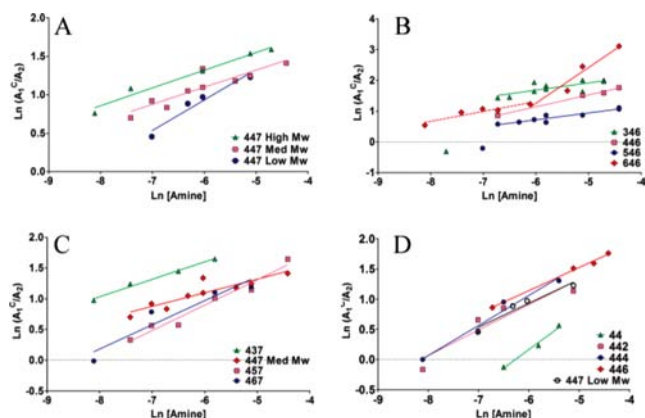
Figure 3. Hill plots for polymer series with varying (A) M_w, (B) backbone, (C) side chain, and (d) end caps.

associated with negative- and positive-cooperativity phases, which may explain why polymer 646 saturated at 96%.

This biphasic nature of binding suggests a change in the binding mechanism increasing amine/phosphate molar ratio (N/P). The analysis and discussion of polymer 646 will focus on the positive-cooperativity slope associated with higher N/P, as all of the other experiments (i.e., transfection, toxicity, diameters, etc.) were carried out at w/w ratios of 30, 60, or 90 (N/P > 35). Polymers 346 and 546 (Figure 3B) have a data point that may be either an outlier or associated with a biphasic binding mechanism similar to that for polymer 646. The fact that there were too few data points in these regions where there may be positive cooperativity for polymers 346 and 546 restricted further analysis. The multiphase cooperativity is an interesting aspect for future investigation.

As the molecular weight of 447 increased, the binding constant per amine (K) increased (Figure 4A). Thus, a larger polymer molecular weight led to increased polymer−DNA interactions and stronger binding. By utilizing this trend, one could potentially fractionate a polymer with a particular molecular weight corresponding to a desired binding constant.
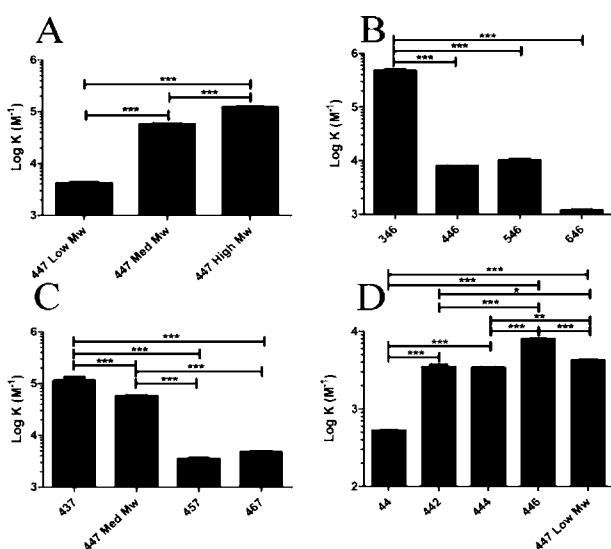

Figure 4. Binding constants (M^{-1}) for the series with varying (A) M_w, (B) backbone, (C) side chain, and (D) end caps. Statistical analysis was accomplished by a one-way ANOVA and a Tukey posthoc analysis: *, $P < 0.05$; **, $P < 0.01$; ***, $P < 0.001$.

When the effect of the number of carbons in the monomer backbone (n_B = 3, 4, 5, or 6) was evaluated, the binding constants decreased as n_B increased (Figure 4B). The binding affinity was reduced 400-fold when n_B increased from 3 to 6. The decrease in the binding constant is likely due to the decrease in amine density with increasing n_B.

The binding constants in the side-chain series (437, 447 Med M_w, 457, 467) decreased with increasing side-chain length n_S (Figure 4C). As the number of carbons in the side chain was increased from 3 to 6, the binding affinity was reduced 24-fold. Again, the decrease in the binding constant is likely due to the decrease in amine density as n_S increases.

The base polymer (polymer 44) had a smaller binding constant than any of the end-capped polymers (442, 444, 446, and 447 Low M_w). The binding constant increased by factors of 6.6 ± 0.1, 15.2, and 8.0 when the base polymer was end-capped using primary (442 and 444), secondary (446), and tertiary amines (447 Low M_w), respectively (Figure 4D). Considering the pK_a values of primary, secondary, and tertiary amines, one would suspect that there would be greater binding for primary versus tertiary amine end caps; however, these differences would be diminished as the buffer pH was 5.2. We observed a larger K value than expected for polymer 446. This larger K value is understandable when the molecular weight of the 446 polymer is considered: the molecular weight of the 446 polymer was 14% higher than the other molecular weights in the end-cap polymer series (Table S1 in the Supporting Information) and thus had 3−5 more amines per polymer strand than the other polymers in the group (the non-end-capped and primary, secondary, and tertiary amine-capped polymers had 40, 39, 44, and 41 amines per polymer strand, respectively).

Comparison of Binding Constant Calculation Methodology. The binding constant of the cationic peptide $(KK)_2KGGC$ was also evaluated to compare our time-resolved fluorescence spectroscopy binding assay to other binding assays found in the literature. The proportion of bound DNA (B in eq 5 in the Supporting Information) as a function of $(KK)_2KGGC$ concentration displayed a saturation level close to 90%. The Hill plot of the peptide presented in Figure S3 in the Supporting Information shows the presence of two phases, similar to the case for polymer 646. The kink point corresponds to a w/w ratio of 3.6. The peptide, perhaps because of the presence of positive cooperativity (at low w/w ratio), was associated with a higher saturation than most of the PBAEs, similar to what was observed with polymer 646. The Hill coefficients of the positive- and negative-cooperativity phases were 2.2 and 0.50, respectively, suggesting that further binding is hindered by the already-bound amines. The overall binding constant K^α obtained from the positive-cooperativity phase was $(1.2 \pm 0.2) \times 10^7$ M^{-1}. Plank et al.[21] obtained a value of 2.09×10^6 M^{-1} with this peptide, which is ~6 times smaller than obtained by our method.

Relationship Between Polyplex Diameter and Binding. The mean diameters of the polyplexes (nanoparticles) formed through binding and self-assembly of cationic polymers with anionic DNA ranged from 122 to 227 nm (Figures S4 and S5 in the Supporting Information). While a polymer with one of the smallest binding constants (646, 1.19×10^3 M^{-1}) formed polyplexes of the largest size (227 nm) and the polymer with the largest binding constant (346, 4.8×10^5 M^{-1}) formed polyplexes of the smallest size (122 nm), there was not an overall trend between the PBAE−DNA binding affinity and the

polyplex size (Figure S4). For the case of polymer backbone length, there was an apparent decrease in the diameter as the binding constant increased (or as the backbone lengths decrease; Figure S4B). As the backbone length increase, the amine density decreases and the hydrophobicity increases as well.

While an increased binding constant appears to correlate with smaller polyplex diameter, the trend is not very strong, as a range of polymer binding constants and polymer structures can produce polyplexes of similar size (Figure S5A). Our data suggest that tighter binding (i.e., larger binding constant) may but does not necessarily result in smaller polymer/DNA polyplexes. The number of plasmids per polyplex, the number of polymer chains per polyplex, and the association of individual polyplexes with each other in ion-containing buffer solutions can all affect the polyplex size.

The polyplex/particle diameter did not appear to show any clear trend in transfection efficacy for either cell line (Figure S5B and S5C). This finding suggests that the diameter of the polymer/DNA polyplexes is not a key determining factor for this class of PBAE particles in these cell lines. As all of the nanoparticles studied were relatively small in diameter, they should be able to mediate successful endocytic cellular uptake.

Polyplexes were successfully formed at both pH values (5.2 and 7.4) and at various ionic strengths (Figure S6 in the Supporting Information). Under these conditions, the diameters of the polyplexes ranged from approximately 100 to 300 nm, and no significant aggregation was observed (Figure S6).

Relationship Between Polyplex ζ Potential and Binding. The polyplexes' ζ potentials (ZPs) (Figures S7 and S8 in the Supporting Information) ranged from +5 to +18 mV. There were no apparent trends between the binding constant and the ZP (Figures S7 and S8A). In contrast to our cationic ZPs, Eltoukhy et al.[18] found that their PBAEs were neutral in sodium acetate, which is likely explained by the use of different polymer structures as well as formulations with w/w ratios of 20−40, which use less polymer than what was tested in our experiments (w/w ratio = 60). Our nanoparticles were weakly positively charged, allowing interaction with a cell's anionic surface. Their charge was not excessive, and they did not cause high toxicity when added to cells. Comparison of the ZP measurements against transfection efficacies revealed no clear trends for either cell line (Figure S8B,C).

These findings suggest that the ZP of the polymer/DNA particles is not a key determining factor for transfection for this class of PBAE particles in these cell lines. As all of the nanoparticles studied were relatively weakly positive in ZP, they should be able to mediate successful cellular uptake.

The ZP of the polyplexes at both pH values (5.2 and 7.4) and at various ionic strengths ranged from approximately +6 to +25 mV (Figure S9 in the Supporting Information). The ZP appeared to be inversely proportional to pH. At pH 5.2, the ZP decreased as the salt content increased. At pH 7.4, the ZP did not appear to increase in all cases as the salt content decreased (Figure S9). The ZPs at 1:100 dilution were comparable to those for the undiluted case.

Effect of Binding Constant on Transfection Efficacy. Two human cancer cell lines (MDA-MB-231 and GBM319) were utilized in these experiments to evaluate the transfection efficacy. The former is derived from invasive triple-negative human breast cancer and the latter is from human glioblastoma multiforme (GBM). Generally speaking, we found both cell lines to be difficult to transfect, with MDA-MB-231 (Figure

5A,C,E,G) being more difficult to transfect than GBM319 (Figure 5B,D,F,H). The relative amount of enhanced green fluorescent protein (EGFP) per cell according to the normalized mean fluorescence was linearly correlated with the transfection efficacy as measured by percent of cells with EGFP (Figure S10 in the Supporting Information).

The optimal molecular weight of the 447 polymer that resulted in the highest transfection efficacy was polymer 447 Med M_w at a w/w ratio of 90 in both cell lines (Figure 5A,B).
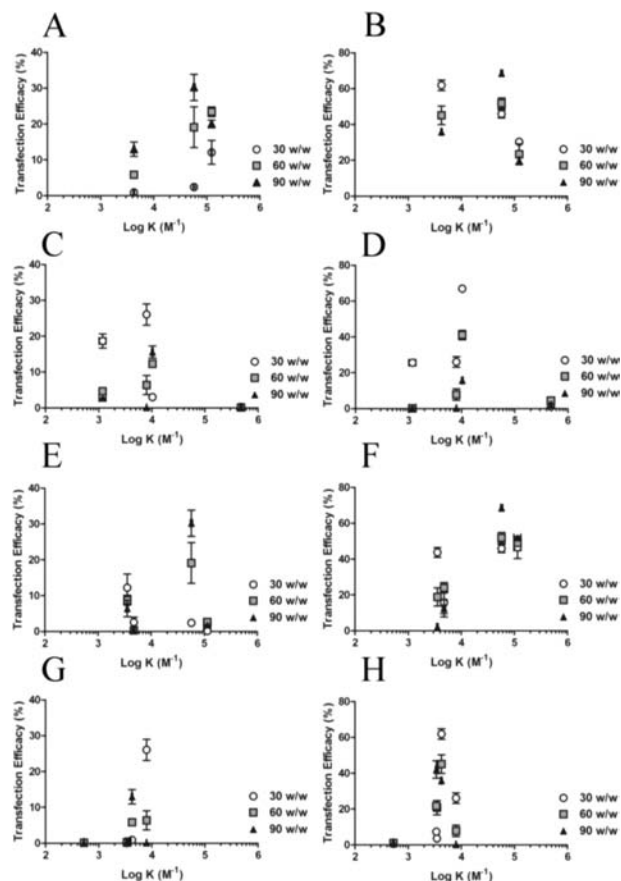

Figure 5. Effect of binding constant on transfection efficacy in (A, C, E, G) MDA-MB-231 cells and (B, D, F, H) GBM319 cells for the series with varying (A, B) M_w, (C, D) backbone, (E, F) side chain, and (G, H) end caps.

By flow cytometry, the 447 Med M_w polymer achieved $30 \pm 4\%$ and $69 \pm 1\%$ transfection in the MDA-MB-231 and GBM319 cell lines, respectively. In MDA-MB-231 cells, the PBAE nanoparticle formulation with the highest transfection efficacy achieved 74% of the transfection percentage achieved with Lipofectamine 2000, a highly effective positive control widely used in the nonviral gene delivery community; positive and negative controls can be found in Figure S11 in the Supporting Information. In GBM319 cells, the leading PBAE nanoparticles transfected 240% of the amount achieved with Lipofectamine 2000. Naked DNA (i.e., the same dose of plasmid DNA without added polymer) resulted in no transfection in either cell line.

When all of the binding constants were analyzed with the transfection efficacy, a biphasic trend was observed, with the peak transfection occurring at an intermediate binding affinity (Figure S12A,B in the Supporting Information). However, the

correlation is not straightforward, as similar binding affinities can also lead to dramatically lower transfection. This is to be expected because binding constants alone are likely insufficient to predict whether a particular polymer will deliver DNA successfully, as there are many factors that affect gene delivery such as cellular uptake, endosomal escape, DNA release, and nuclear import (Scheme 1).[5]

I. Effect of M_w. In the MDA-MB-231 cells, a comparison of the 447 polymers with incremental molecular weight (Figure 5A) revealed a biphasic response, with the highest transfection efficacy occurring at intermediate polymer molecular weight (447 Med M_w) and intermediate binding affinity (58 000 M^{-1}). For the w/w ratio = 30 group, there was an increase in transfection efficacy for the MDA-MB-231 cell line as the molecular weight increased (Figure 5A), whereas there was a decrease for the GMB319 cell line (Figure 5B). Polymer 447 Med M_w with a binding constant of 58 000 M^{-1} was the most effective polymer evaluated in terms of transfection efficacy for the GBM319 cells (Figure 5B). This suggests that there is an optimal range: having a binding constant that is either too small or too large is unfavorable. Polymers with small binding constants may not be able to condense and protect the DNA sufficiently, and ones with excessively large binding constants likely do not release the DNA as efficiently.[22] As the molecular weight increased from 10.3 to 91.6 kDa, the transfection efficacy decreased from approximately 60% to 30% positive cells in the GBM319 cells.

II. Effect of Single Carbon Differences. When the molecular weight was held approximately constant and the backbone and side chain were varied, the optimal binding constant was near 58 000 M^{-1} (polymer 447 Med M_w) for MDA-MB-231 cells (Figure 5C,E), and the transfection was similarly high (~70%) for GBM319 cells for binding constants in the range (1−6) × 10^4 M^{-1} (Figure 5D,F). In cases where the binding constant is smaller than 10^4 M^{-1}, increasing the binding constant correlates with increased transfection efficacy for MDA-MB-231 cells. GBM319 cells are better transfected by polymers with smaller binding constants (10^3−10^4 M^{-1}) than the MDA-MB-231 cells are, and this is likely due to intrinsic differences in the gene delivery transport steps (Scheme 1) for these two cell types. For both cell types, when the binding constant increased further (>10^5 M^{-1}), even at constant molecular weight, transfection decreased.

Although it is common practice to use 10% fetal bovine serum for in vitro transfection experiments, higher media serum content may be more physiologically relevant. When 70% serum was used to assess the transfection efficacy and its correlation with the observed binding constants in the GBM319 cell line, the highest transfection achieved in the presence of high serum was similar to that observed with low serum, approximately 70% of human cells positively transfected. A biphasic trend similar to that under 10% serum conditions was also observed (Figure S13 in the Supporting Information), and a similar optimal range of binding constants, ~10^4 M^{-1}, was able to result in the highest transfection efficacy.

III. Effect of End Caps. The MDA-MB-231 and GBM319 cell lines had very low transfection for the non-end-capped, acrylate-terminated polymer (polymer 44). Furthermore, the primary-amine-capped polymers (polymers 442 and 444) were not able to transfect MDA-MB-231 cells effectively, whereas polymers capped with primary, secondary, and tertiary amines were able to transfect the GB319 cells.

Secondary or tertiary amine end caps, depending on the w/w ratio, were required for effective transfection of the MDA-MB-231 cell line with these polymers. The GBM319 cell line could be successfully transfected via PBAE polymers end-capped with primary amines (442 and 444) in addition to the polymers end-capped with secondary or tertiary amines. However, there did not appear to be a strong trend with the binding constant and transfection efficacy in the end-capped series (Figure 5G,H).

Effect of Binding Constant on Cytotoxicity. In general, the cytotoxicity increased with increasing polymer/DNA w/w ratio (Figure 6). In both cell lines tested, it appeared that there
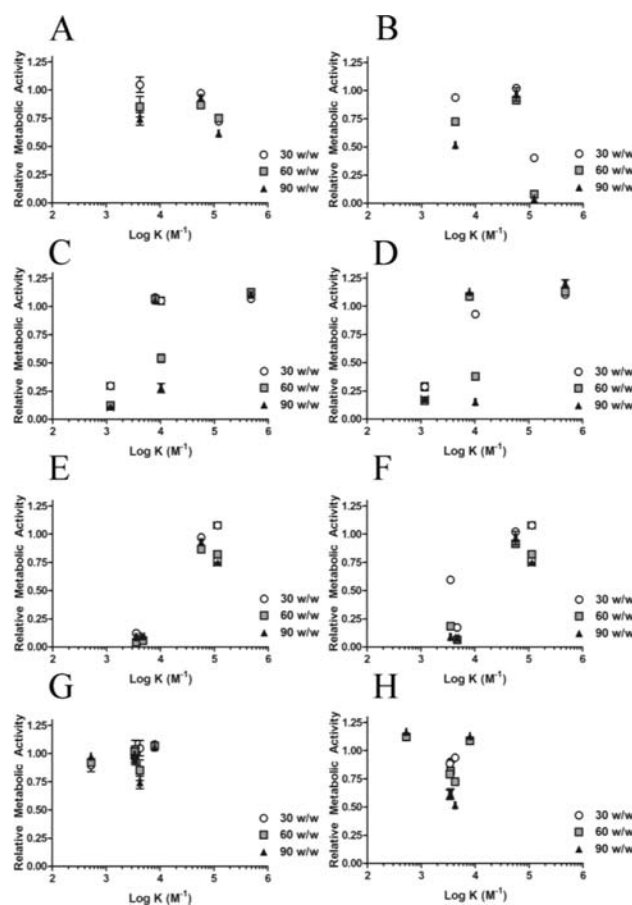

Figure 6. Effect of binding constant on relative metabolic activity in (A, C, E, G) MDA-MB-231 cells and (B, D, F, H) GBM319 cells for the series with varying (A, B) M_w, (C, D) backbone, (E, F) side chain, and (G, H) end caps.

was low cytotoxicity with polymers that had binding constants in the 10^4−10^5 M^{-1} range (Figure S12C,D in the Supporting Information).

I. Effect of M_w. Particle-induced cytotoxicity in both cell lines increased as the binding constant (and M_w) increased (Figure 6A,B). There was relatively less toxicity in the MDA-MB-231 cell line than in the GB319 cell line, especially for the 447 High M_w polymer.

II. Effect of Single Carbon Differences. The cytotoxicity in both cell lines increased as the number of carbons in the backbone or side chain increased. Thus, the cytotoxicity decreased (and the relative metabolic activity increased) as the binding constant increased (Figure 6C−F).

III. Effect of End Caps. There was no significant cytotoxicity in the MDA-MB-231 cell line with the 44, 442, 444, 446, and

447 Low end-cap series, whereas there appeared to be some cytotoxicity in the GBM319 cell line with the primary and tertiary amine end caps. Secondary amine end caps may be particularly less cytotoxic in the GBM319 cell line (Figure 6G,H). There was not a clear trend in the relative metabolic activity when the type of end cap was varied.

Heparin Competition Release. The 44 polymer associated with the weakest binding constant (526 M^{-1}) released its DNA with the lowest amount of heparin (<2 μg/mL) (Figure S14 in the Supporting Information). Polymer 447 Low M_w was associated with a binding constant of 4.2×10^3 M^{-1} and released its DNA at a heparin concentration between 16 and 64 μg/mL (Figure S14). The 446 and 447 High M_w polymers were associated with binding constants of 7.97×10^3 and 1.23×10^5 M^{-1}, respectively, and both released their DNA at heparin concentrations between 128 and 256 μg/mL. The 446 polymer exhibited a faint supercoiled DNA band at 128 μg/mL, suggesting that this polymer likely releases its DNA at a lower heparin concentration than does 447 High M_w (Figure S14). The DNA release from the polyplexes appeared to be inversely proportional to the binding affinity between DNA and the polymers.

CONCLUSIONS

Evaluation of polymer−DNA binding constants using time-correlated single-photon counting and comparison of these values to transfection efficacies allowed us to observe that binding constants of $(1-6) \times 10^4$ M^{-1} were optimal for both human cancer cell lines tested. Our data reveal that the polymer−DNA binding affinity for PBAEs is biphasic with respect to transfection efficacy, with an intermediate binding affinity being optimal. A binding constant in the optimal range is necessary but not sufficient for effective transfection. This intermediate binding affinity can be independently tuned by adding single carbons to the backbone or side-chain structure, by varying the monomer ratio during synthesis and/or using GPC fractionation to tune the polymer molecular weight, and by modifying a small-molecule end group used to end-cap a linear polymer. Probing a specific gene delivery bottleneck with a class of polymers that were synthesized to have subtle structural differences has revealed new quantitative and mechanistic insights concerning how they function for gene delivery.

ASSOCIATED CONTENT

Ⓢ Supporting Information

Materials and methods; ^{1}H NMR spectra of polymers 44, 442, 444, 446, and 447 (Figure S1); decay-associated spectra (Figure S2); lists of M_n, M_w, PDI, degree of polymerization, Hill coefficient, K, diameter, and ZP for the studied polymers (Table S1); peptide Hill plot (Figure S3); plots of diameter versus binding constant for various polymer series (Figure S4); plots of diameter versus binding constant and transfection efficacy versus diameter (Figure S5); figure of polyplex diameters at various pHs and ionic strengths (Figure S6); plots of ZP versus binding constant for various polymer series (Figure S7); plots of ZP versus binding constant and of transfection efficacy versus ZP (Figure S8); figure of polyplex ZP at various pHs and ionic strengths (Figure S9); correlations between geometric and arithmetic mean fluorescences (FL1-A) and percent positive transfection efficacies in both cell lines (Figure S10); positive and negative controls for transfection and relative metabolic activity (Figure S11); plots of binding constants and relative metabolic activities versus transfection efficacy (Figure S12); plot of transfection efficacy versus binding constant in 70% serum for the GBM319 cell line (Figure S13); and heparin release competition assay via gel electrophoresis (Figure S14). This material is available free of charge via the Internet at http://pubs.acs.org.

AUTHOR INFORMATION

Corresponding Author
green@jhu.edu
Notes
The authors declare no competing financial interest.

ACKNOWLEDGMENTS

REFERENCES

(1) Nielsen, L. L.; Maneval, D. C. *Cancer Gene Ther.* **1998**, *5*, 52.
(2) Ziady, A. G.; Kelley, T. J.; Milliken, E.; Ferkol, T.; Davis, P. B. *Mol. Ther.* **2002**, *5*, 413.
(3) Thomas, M.; Klibanov, A. M. *Appl. Microbiol. Biotechnol.* **2003**, *62*, 27.
(4) Pearson, S.; Jia, H. P.; Kandachi, K. *Nat. Biotechnol.* **2004**, *22*, 3.
(5) Sunshine, J. C.; Bishop, C. J.; Green, J. J. *Ther. Delivery* **2011**, *2*, 493.
(6) Sunshine, J. C.; Akanda, M. I.; Li, D.; Kozielski, K. L.; Green, J. J. *Biomacromolecules* **2011**, *12*, 3592.
(7) Green, J. J. *Ann. Biomed. Eng.* **2012**, *40*, 1408.
(8) Green, J. J.; Langer, R.; Anderson, D. G. *Acc. Chem. Res.* **2008**, *41*, 749.
(9) Shmueli, R. B.; Sunshine, J. C.; Xu, Z. H.; Duh, E. J.; Green, J. J. *Nanomedicine (New York)* **2012**, *8*, 1200.
(10) Sunshine, J.; Green, J. J.; Mahon, K. P.; Yang, F.; Eltoukhy, A. A.; Nguyen, D. N.; Langer, R.; Anderson, D. G. *Adv. Mater.* **2009**, *21*, 4947.
(11) Tzeng, S. Y.; Guerrero-Cazares, H.; Martinez, E. E.; Sunshine, J. C.; Quinones-Hinojosa, A.; Green, J. J. *Biomaterials* **2011**, *32*, 5402.
(12) Bhise, N. S.; Shmueli, R. B.; Gonzalez, J.; Green, J. J. *Small* **2012**, *8*, 367; Corrigendum: **2012**, *8*, 1129.
(13) Akinc, A.; Lynn, D. M.; Anderson, D. G.; Langer, R. *J. Am. Chem. Soc.* **2003**, *125*, 5316.
(14) Akinc, A.; Langer, R. *Biotechnol. Bioeng.* **2002**, *78*, 503.
(15) Sunshine, J. C.; Peng, D. Y.; Green, J. J. *Mol. Pharmaceutics* **2012**, *9*, 3375.
(16) Sunshine, J. C.; Sunshine, S. B.; Bhutto, I.; Handa, J. T.; Green, J. J. *PloS One* **2012**, *7*, No. e37543.
(17) Huang, Y. H.; Zugates, G. T.; Peng, W.; Holtz, D.; Dunton, C.; Green, J. J.; Hossain, N.; Chernick, M. R.; Padera, R. F., Jr.; Langer, R.; Anderson, D. G.; Sawicki, J. A. *Cancer Res.* **2009**, *69*, 6184.
(18) Eltoukhy, A. A.; Siegwart, D. J.; Alabi, C. A.; Rajan, J. S.; Langer, R.; Anderson, D. G. *Biomaterials* **2012**, *33*, 3594.
(19) Wang, J.; Gao, S. J.; Zhang, P. C.; Wang, S.; Mao, M. Q.; Leong, K. W. *Gene Ther.* **2004**, *11*, 1001.
(20) Zelikin, A. N.; Trukhanova, E. S.; Putnam, D.; Izumrudov, V. A.; Litmanovich, A. A. *J. Am. Chem. Soc.* **2003**, *125*, 13693.
(21) Plank, C.; Tang, M. X.; Wolfe, A. R.; Szoka, F. C., Jr. *Hum. Gene Ther.* **1999**, *10*, 319.
(22) Schaffer, D. V.; Fidelman, N. A.; Dan, N.; Lauffenburger, D. A. *Biotechnol. Bioeng.* **2000**, *67*, 598.

(23) Leong, K. W.; Mao, H. Q.; Truong-Le, V. L.; Roy, K.; Walsh, S. M.; August, J. T. *J. Controlled Release* **1998**, *53*, 183.

(24) Tam, P.; Monck, M.; Lee, D.; Ludkovski, O.; Leng, E. C.; Clow, K.; Stark, H.; Scherrer, P.; Graham, R. W.; Cullis, P. R. *Gene Ther.* **2000**, *7*, 1867.

(25) Yu, R. Z.; Geary, R. S.; Leeds, J. M.; Watanabe, T.; Fitchett, J. R.; Matson, J. E.; Mehta, R.; Hardee, G. R.; Templin, M. V.; Huang, K.; Newman, M. S.; Quinn, Y.; Uster, P.; Zhu, G.; Working, P. K.; Horner, M.; Nelson, J.; Levin, A. A. *Pharm. Res.* **1999**, *16*, 1309.

(26) Green, J. J.; Zugates, G. T.; Tedford, N. C.; Huang, Y. H.; Griffith, L. G.; Lauffenburger, D. A.; Sawicki, J. A.; Langer, R.; Anderson, D. G. *Adv. Mater.* **2007**, *19*, 2836.

(27) van der Aa, M. A. E. M.; Huth, U. S.; Hafele, S. Y.; Schubert, R.; Oosting, R. S.; Mastrobattista, E.; Hennink, W. E.; Peschka-Suss, R.; Koning, G. A.; Crommelin, D. J. A. *Pharm. Res.* **2007**, *24*, 1590.

(28) Ketola, T. M.; Hanzlikova, M.; Urtti, A.; Lemmetyinen, H.; Yliperttula, M.; Vuorimaa, E. *J. Phys. Chem. B* **2011**, *115*, 1895.

(29) Vuorimaa, E.; Ketola, T. M.; Green, J. J.; Hanzlikova, M.; Lemmetyinen, H.; Langer, R.; Anderson, D. G.; Urtti, A.; Yliperttula, M. *J. Controlled Release* **2011**, *154*, 171.

(30) Vuorimaa, E.; Urtti, A.; Seppanen, R.; Lemmetyinen, H.; Yliperttula, M. *J. Am. Chem. Soc.* **2008**, *130*, 11695.